Construction of Symbolic Dynamics from Experimental Time Series

K. Mischaikow*

School of Mathematics, Georgia Institute of Technology, Atlanta, Georgia 30332

M. Mrozek†

Instytut Informatyki, Uniwersytet Jagielloński, 30-072 Kraków, Poland

J. Reiss‡

School of Physics, Georgia Institute of Technology, Atlanta, Georgia 30332

A. Szymczak§

School of Mathematics, Georgia Institute of Technology, Atlanta, Georgia 30332

Symbolic dynamics play a central role in the description of the evolution of nonlinear systems. Yet there are few methods for determining symbolic dynamics of chaotic data. One difficulty is that the data contains random fluctuations associated with the experimental process. Using data obtained from a magnetoelastic ribbon experiment we show how a topological approach that allows for experimental error and bounded noise can be used to obtain a description of the dynamics in terms of subshift dynamics on a finite set of symbols. [S0031-9007(99)08415-X]

There has been considerable effort within the scientific community to develop methods to determine whether a given dynamical system is chaotic [1]. Three issues make rigorous analysis of chaotic dynamics difficult: global nonlinearities making it difficult to obtain the necessary analytic estimates; trajectories are inherently sensitive to the initial conditions; the objects of interest, namely, invariant sets, can undergo dramatic changes in their structure due to local and global bifurcations. The problem is dramatically more complicated in the setting of experimental systems because of the introduction of noise, parameter drift, and experimental error.

In a recent paper [2] we introduced new topological techniques designed to overcome these difficulties. In this paper, these techniques are successfully applied in the context of an actual physical system, a magnetoelastic ribbon subject to a periodically oscillating magnetic field. Our ideas are extensions of the numerical methods developed in [3,4] along with a reinterpretation of what is an appropriate embedding theorem [5–7] to justify the use of time delay reconstructions.

At the basis of our approach are three assumptions. The first is that the dynamics of the physical system can be represented by a continuous map $f : X \times \Lambda \to X$, where X represents the phase space and Λ represents the experimentally relevant range of parameter space. The second assumption is that we are trying to describe the dynamics of an attractor for f in X. The third involves the relationship between the physical phase space and the values observed by the experimentalist. In particular, the experimental observation is represented as a multivalued map $\theta : X \to [\alpha_x, \beta_x] \subset \mathbf{R}$, where $|\alpha_x - \beta_x|$ may be thought of as an upper bound for the experimental error.

We assume that there is a continuous map $\gamma : X \to \mathbf{R}$ such that $\gamma(x) \in \theta(x)$ for all $x \in X$. One may view γ as representing the "true" measurement of the system. We are only assuming the existence of such a γ, but *never* assume that it is known. Observe that, if it is impossible to choose θ and γ as above, for some points in the physical phase space arbitrarily small changes in the physical system must lead to arbitrarily large changes in measurements.

Recall that a *transition matrix A* on k symbols is a $k \times k$ matrix whose entries a_{ij} take values of 0 or 1. Given A, one can define a subset of the set of bi-infinite sequences on k symbols, $\Sigma_A := \{s = (s_n) \mid s_n \in \{1, 2, \ldots, k\}$ and $a_{s_n, s_{n+1}} = 1\}$. Let $\sigma : \Sigma_A \to \Sigma_A$ denote the shift dynamics, $\sigma(s)_n = s_{n+1}$.

If the dimension of the reconstruction space is d, then applying our method results in regions N_i, $i = 1, \ldots, k$ in $\mathbf{R}^d$ and a $k \times k$ transition matrix A for which the following conclusion can be justified [2]. Given any sequence $\{\lambda_n\} \subset \Lambda$ and any element $s \in \Sigma_A$, there exists an initial condition $x \in X$ such that, for all $n = 1, 2, \ldots,$

$$\theta(f^n(x, \lambda_n)) \times \theta(f^{n+1}(x, \lambda_{n+1})) \times \cdots \times$$
$$\theta(f^{n+d}(x, \lambda_{n+d})) \cap N_{s_n} \neq \varnothing.$$

In other words, given any sequence of perturbations in the parameter settings, there exists an initial condition such that, up to experimental error, the reconstructed dynamics describes the observed physical dynamics.

Experimental setup.—The magnetoelastic ribbon is a thin strip of material with the property that its Young's modulus varies with the strength of an applied magnetic field. A region of uniform field was created by the use of three Helmholtz coils. The ribbon was placed in this field

and clamped from the bottom. The ribbon and Helmholtz coils were placed upon a vibration isolation table and the entire apparatus was in a temperature-controlled, sealed room, thereby minimizing environmental effects. Nevertheless, the system was extremely sensitive, and thus a significant amount of error was taken into account when performing the calculations. An oscillating magnetic field was applied vertically. When the magnetic field strength is within a certain range, the ribbon will buckle under its own weight. Under these conditions, the ribbon will oscillate back and forth as its stiffness changes. Depending upon the strength and frequency of the applied oscillating field, as well as the physical characteristics of the ribbon, the motion of the ribbon can exhibit a wide variety of different behaviors. The position of the ribbon once per driving period was investigated.

The data set consisted of 100 000 consecutive data points $\{v_n \mid n = 1, \ldots, 100\,000\}$ taken from voltage readings on the photonic sensor, sampled at the drive frequency of 1.2 Hz. The readings were measured up to 10^{-3} volts.

Implementation of our method.—We selected 30 000 data points $\{v_n \mid n = 30\,000, \ldots, 60\,000\}$ from our data set and chose a reconstruction dimension of 2 producing the reconstruction plot of $U := \{u_n = (v_n, v_{n+1})\} \subset \mathbf{R}^2$ indicated in Fig. 1. We divided $\mathbf{R}^2$ into a grid of squares with each side of length 0.0106 volts. $\mathcal{G}$ is the set of squares which contain a point $u_n \in U$, and $Y \subset \mathbf{R}^2$ is the region determined by this collection of squares (see Fig. 2).

The next step is to define a dynamical system on Y that captures the observable dynamics of the experiment. Since the physical system is subject to noise and experimental error, we do not describe the dynamics on any scale smaller than that of the squares in $\mathcal{G}$, and our dynamical system has the form of a multivalued map $\mathcal{F}$ taking squares to sets of squares. To be more precise, let $G \in \mathcal{G}$ and let $\{u_{\alpha_i} \mid i = 1, 2, \ldots, I\} \subset U$ be the set of points which lie in G. Let $G_i' \in \mathcal{G}$ such that $u_{\alpha_i+1} \in G_i'$. Up to first approximation we require that $G_i' \in \mathcal{F}(G)$. Unfortunately, this definition is not sufficient.
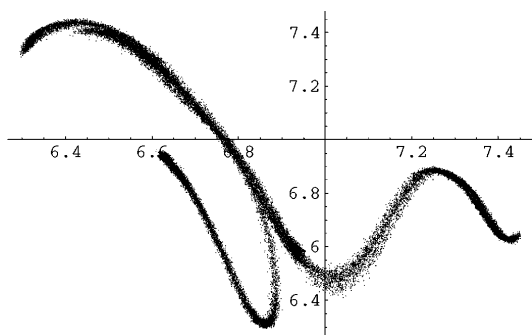
One reason is that there may be few samples in G, so that $G_1', G_2', \ldots, G_I'$ are isolated squares far apart from each other. $\mathcal{F}(G)$ should be a connected set and capture all possible images of points of G, not just the ones for which we have samples from the time series. Therefore, all grid squares contained in the smallest rectangle enclosing $G_1', G_2', \ldots, G_I'$ in $\mathcal{F}(G)$ are included. This may still not be enough, since the images of four squares meeting at one point may not intersect, preventing the map $\mathcal{F}$ from having a continuous selector. We deal with this problem in the following way. For each grid point, look at the images of the four grid squares which meet at that point. If they do not intersect, increases each image by the set of all squares which intersect the set representing it. Repeat this process until there are no empty intersections. Finally, intersect each image of a grid square with $\mathcal{G}$. This procedure constructs a multivalued map $\mathcal{F}$ on $\mathcal{G}$ which we believe provides outer limits on the observable dynamics of the experimental system. Trajectories in this dynamical system consist of sequences of squares of the form $\{G_i \in \mathcal{G} \mid G_{i+1} \in \mathcal{F}(G_i)\}$.

To discuss the issue of which dynamics is represented by $\mathcal{F}$ requires several slight theoretical digressions. Let $g : \mathbf{R}^n \to \mathbf{R}^n$ be an arbitrary continuous map. Recall that $S \subset \mathbf{R}^n$ is an *invariant set* of g if, for every $x \in S$, there exists a bi-infinite sequence $\{x_i\} \subset S$ such that $x = x_0$ and $x_{i+1} = g(x_i)$. While invariant sets are the object of interest in dynamical systems, they can be extremely difficult to study directly since they may change their properties dramatically through various local or global bifurcations. For this reason we shall make use of the following notion. A closed bounded set $N \subset \mathbf{R}^n$ is an *isolating neighborhood* if the maximal invariant set in N does not intersect the boundary of N. If N is an isolating neighborhood for the dynamical system generated by g, then it is an isolating neighborhood for sufficiently small perturbations of g.

FIG. 1. Time delay plot of $u_n = (v_n, v_{n+1})$, $n = 30\,000$, $\ldots, 60\,000$, where v_n is the nth voltage.

FIG. 2. Squares with edges of length 0.0106 volts that contain points $u_n \in U$ of the time delay reconstruction.

Returning to the magnetoelastic ribbon we now look for isolating neighborhoods in Y under the multivalued dynamical system $\mathcal{F}$. There are a variety of criteria that can be used in choosing $C_0 \subset \mathcal{G}$; the important point is that it must be a strict subset of $\mathcal{G}$. We used the following procedure. Define $C_1 = C_0 \cap \mathcal{F}(C_0) \cap \mathcal{F}^{-1}(C_0)$, where $\mathcal{F}^{-1}(C_0) := \{G \in \mathcal{G} \mid \mathcal{F}(G) \cap C_0 \neq \varnothing\}$. Delete a component of C_1 which touches the boundary of C_0 relative to Y. This two step procedure is repeated until $C_{n+1} = C_n$. The resulting set C_n is an isolating neighborhood for $\mathcal{F}$ (see Fig. 3). Observe that C_n consists of four disjoint sets labeled N_i, $i = 1, \ldots, 4$.

We will use the Conley index theory [8] to resolve the following theoretical issue: While isolating neighborhoods can be computed, it is the structure of the corresponding isolating invariant set which is of interest. Given an isolating neighborhood N of g, a pair of closed bounded sets (K, L) with $L \subset K \subset N$ is an *index pair* if the following conditions are satisfied: (1) $x \in K$ and $g(x) \in N$, then $g(x) \in K$; (2) $x \in L$ and $g(x) \in N$, then $g(x) \in L$; (3) $x \in K$ and $g(x) \notin N$, then $x \in L$; (4) the maximal invariant set in N is a subset of the interior of K excluding L. The importance of an index pair is that the homology groups $H_*(K, L)$ and a homology map $\tilde{g}_* : H_*(K, L) \rightarrow H_*(K, L)$ induced by g are invariants of the maximal invariant set contained in N. Also, if under a change in the dynamics, N remains an isolating neighborhood, the homology group and map do not change.

We produce an index pair for $\mathcal{F}$ as follows. Let L consist of the elements of $\mathcal{F}(C_n)$ which touch the boundary of C_n relative to Y. Let $K = C_n \cup L$. Then (K, L) is an index pair for $\mathcal{F}$. Figure 3 indicates the resulting index pair.

We now compute $H_*(K, L)$ using $\mathbf{Z}_2$ coefficients and determine that it is a four-dimensional vector space and the corresponding map on homology is the matrix in Fig. 3.

The embedding theorems of [5–7] assume that the points $U \subset \mathbf{R}^2$ actually represent elements of trajectories of a fixed smooth map on a subset of $\mathbf{R}^2$ and that the dynamics of this map can now be embedded into the dynamics of the physical system. Observe that we make no such assumption. Instead we use the existence of the continuous map $\gamma : X \rightarrow \mathbf{R}$ to lift the algebraic topological quantities associated with A to X. This allows one to conclude [2] that A represents a transition matrix for a symbolic coding of the dynamics in the physical phase space.

This implies that, given any small random environmental effects on the experiment and any sequence $b \in \Sigma_A$, there exists an initial condition for the physical system such that, using our observational method, the trajectory will, up to experimental error, pass through the regions labeled N_i, $i = 1, \ldots, 4$ in the manner indicated by b.

Conclusions.—Our method provides an explicit symbolic dynamics description of the chaotic behavior of the magnetoelastic ribbon. This is a finer information than usual from experimental data. For example, given A it is easy to conclude that the topological entropy for the ribbon must be greater than $\ln 1.4656$.

Two other methods that are commonly used to analyze chaotic data involve the approximation of Lyapunov exponents or the determination of a fractal dimension. These methods and ours require similar assumptions: (1) The data provided is a reasonable approximation to what one would obtain if measurements could be performed for an infinite amount of time; (2) the phase space reconstruction has given a good approximation to the underlying dynamics; (3) the underlying system is assumed to be governed by a deterministic set of equations.

For the computation of Lyapunov spectra, one must assume that the reconstruction has been done in a sufficiently high-dimensional space. In our setting this is not necessary, whenever one computes nontrivial algebraic topological quantities the resulting conclusions about the dynamics are correct. If one chooses too low a dimension, the algebra corresponding to the resulting
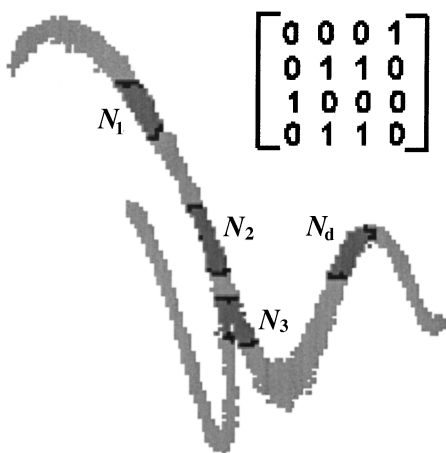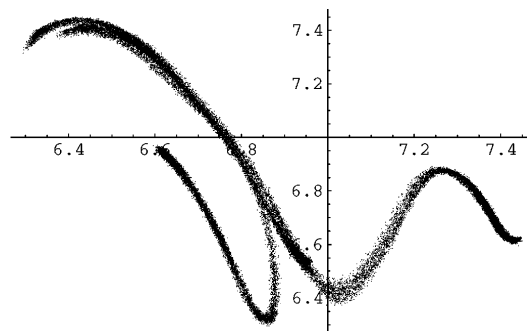

FIG. 3. Results from the data points 30 000 through 60 000. The four shaded regions labeled $N_1, \ldots, N_4$ make up the set C_n. Darkly shaded regions on the boundary of the N_i are L.

FIG. 4. Time delay plot of $u_n = (v_n, v_n + 1)$, $n = 70\,000$, $\ldots, 100\,000$, where v_n is the nth voltage.
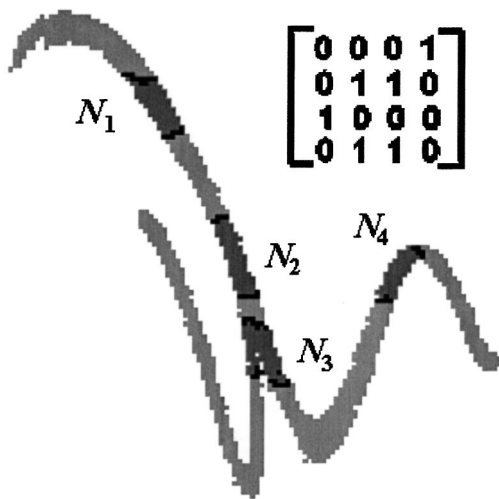
FIG. 5. Results from the data points 70 000 through 100 000. The four shaded regions labeled $N_1, \ldots, N_4$ make up the set C_n. Darkly shaded regions on the boundary of the N_i are L.

multivalued map will be trivial. It is easy to construct examples where an embedding fails but the algebra is still nontrivial. A more fundamental problem is that Lyapunov exponents are sensitive to noise and perturbations, but quantification of this sensitivity is not known.

We performed Lyapunov exponent calculations and embedding dimension calculations on this data set. The dominant Lyapunov exponent seemed to be roughly 0.48. However, under reasonable parameter regimes, the computed Lyapunov exponent ranged between 0.45 and 0.99.

Similar problems exist with a determination of fractal dimension. A reasonable estimate of dimension is difficult to compute from experimental data and the dimension tells little about the underlying dynamics. Measurement of the embedding dimension also yielded somewhat questionable results. One method identifies the percentage of false nearest neighbors for a given embedding dimension. The minimum embedding dimension differed greatly depending on our criteria for identification of a false nearest neighbor. In some analyses, it seemed an embedding dimension of 5 was necessary to decrease the percentage of false nearest neighbors to less than 5%.

Finally, our approach appears to provide robust repeatable conclusions. As was mentioned earlier, we collected 100 000 data points. We repeated the above mentioned procedure using the points $\{v_n \mid n = 70\,000, \ldots, 100\,000\}$. As one can see from Fig. 4, there are observable differences in this collection of data points. After applying our procedure we obtain the index pairs indicated in Fig. 5 which are also slightly different. However, on the level of the algebra and hence the symbolic dynamics, we obtained the same transition matrix.

In conclusion, we have proposed a theoretically justified and experimentally validated method which takes time series as input and produces the output of a transition matrix and its associated regions in reconstruction space which may be used to rigorously verify chaos, analyze and identify invariant sets, and determine properties of the global dynamics above the noise level. All analysis is on a scale where the results of the analysis are robust with respect to noise. Quantitative measurements of chaos may fail because of sensitivity in the analysis. In contrast, verification of chaos from analysis of the transition matrix is robust.

*Electronic address: mischaik@math.gatech.edu
†Electronic address: mrozek@ii.uj.edu.pl
‡Electronic address: jreiss@acl.gatech.edu
§Electronic address: andrzej@math.gatech.edu

[1] H. Abarbanel, *Analysis of Observed Chaotic Data* (Springer, New York, 1996).
[2] K. Mischaikow, M. Mrozek, A. Szymczak, and J. Reiss, preprint, see http://www.math.gatech.edu/~mischaik/papers/paperlist.html
[3] K. Mischaikow and M. Mrozek, Bull. AMS **33**, 66–72 (1995).
[4] K. Mischaikow and M. Mrozek, Math. Comput. **67**, 1023–1046 (1998).
[5] M. Casdagli, T. Sauer, and J. A. Yorke, J. Stat. Phys. **65**, 579–616 (1991).
[6] J.-P. Eckmann and D. Ruell, Rev. Mod. Phys. **57**, 617 (1985).
[7] F. Takens, in *Dynamical Systems and Turbulence, Warwick 1980,* edited by D. Rand and L. S. Young (Springer, Berlin, 1981), p. 366.
[8] L. Arnold, C. Jones, K. Mischaikow, and G. Raugel, in *Dynamical Systems Montecatini Terme 1994,* edited by R. Johnson, Lecture Notes in Mathematics (Springer, New York, 1995), p. 1609.